Variability in the Structures of Luminescent [2-(Aminomethyl)pyridine]silver(I) Complexes: Effect of Ligand Ratio, Anion, Hydrogen Bonding, and π-Stacking

Rodney P. Feazell,[a] Cody E. Carson,[a] and Kevin K. Klausmeyer*[a]

Keywords: Silver / N ligands / X-ray diffraction / Coordination modes

The reaction of 2-(aminomethyl)pyridine (2-amp) with silver(I) salts of triflate (OTf^-), trifluoroacetate (tfa^-), and tetrafluoroborate (BF_4^-) produce monomeric, dimeric, bridged, and polymeric structural motifs. The structural characteristics are dependent upon the ratio of ligand/metal in the structure as well as the ability of the anion to coordinate to the metal centers and form hydrogen bonds to the bound ligands. The silver coordination environment takes on several geometries including near linear (**6**), trigonal (**4**), tetrahedral (**1**), and both trigonal-bipyramidal and square-based pyramidal in a single structure (**2**). Structures **2**, **3**, and **5** also display short Ag–Ag contacts ranging from 2.8958(3) to 3.0305(4) Å. The species with metal–metal interactions, which are connectively very similar to their metal-isolated counterparts of **1**, **4**, and **6**, are held together only by weak π-stacking interactions or hydrogen bonds to their respective anions. Low-temperature luminescence spectra were collected for all compounds and are compared.

Introduction

Progress in the field of crystal engineering has been greatly complemented by coordination studies of the coinage metals.[1–8] Studies of silver in particular have had much to offer. This is because of the flexibility in its coordination sphere and the ease with which it varies the coordination number.[9–13] Many silver coordination architectures are readily obtainable through slight variations in ligand and/or anion and include discrete, small molecules, supramolecular arrays, and 1-, 2-, and 3-dimensional coordination networks.[13–17] Several systematic studies of the structural dependence on anions have been nicely demonstrative of the diversity possible with small changes in counterion properties such as coordinating or hydrogen-bonding ability.[18–23] A related area of this research that has proved lacking, however, is that concerned with the ligand/metal ratio dependence of these structures.[24] To the best of our knowledge, no thorough report has been given that shows the effects of changing the ratio of ligand/metal in bidentate silver(I) systems of various anions. This led us to investigate the changes in the solid-state structures of [2-(aminomethyl)-pyridine]silver(I) complexes that are caused by altering the ratio of ligand/metal in the reaction mixtures. One resulting feature that is of particular interest in these and other silver complexes is the closed-shell metal–metal interaction that is very well known to occur in the monovalent group 11 elements.[25–31] While not as broadly represented or studied as the aurophilic attraction that holds the gold–gold interaction intact, a small surge of recent work has been dedicated to examining the properties of this argentophilic contact.[32–37] Included in this group are a handful of theoretical studies that put the strength of the interaction along the same intensity as that of a hydrogen bond with an idealized internuclear separation of 3.137–3.208 Å.[38–41]

Herein we demonstrate that not only can the molecular architecture of silver(I) coordination complexes be altered by changes in the counterion, but they can also be largely affected by the ratio of ligand/metal. The 2-(aminomethyl)-pyridine ligand, whose small bite angle imposes a predisposition for chelation, is seen to construct a range of coordination motifs, shown in Figure 1, from simple monomers to coordination polymers with various silver(I) salts simply by changing its ratio in solution. The resulting complexes contain a number of interesting structural features and physical properties including several short, sterically unfavored Ag–Ag interactions, bridging 2-amp ligands and a pronounced luminescence.

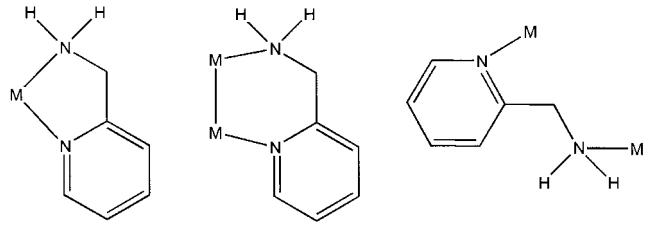

Figure 1. Binding modes that are seen with the 2-(aminomethyl)-pyridine ligand in the silver(I) structures described herein.

[a] Department of Chemistry and Biochemistry, Baylor University, Waco, TX 76798-7348, USA
Fax: +1-254-710-4272
E-mail: kevin_klausmeyer@baylor.edu
Supporting information for this article is available on the WWW under http://www.eurjic.org or from the author.

Results and Discussion

Preparation and NMR Spectroscopy

The 2-(aminomethyl)pyridine complexes **1**–**7** (Schemes 1, 2, and 3) were all prepared by the direct reaction of the ligand with silver(I) salts in varying ratios. The 1:1 $AgBF_4$ structure has already been discussed in a previous study.[23] The many intriguing structural features of the complexes presented here are seen to stem directly from the ratio of ligand/metal, with the ratio itself often being influenced by the properties of the anion present. An example of this is the silver triflate complex which we have been unable to force beyond a 3:2 ratio of ligand/metal, while that of the trifluoroacetate has not been isolable at 3:2 but proceeds directly to 2:1. Hydrogen bonding between the amine protons and the anions are a major determining factor in the structure, orientation, and 3-dimensional growth of the complexes.

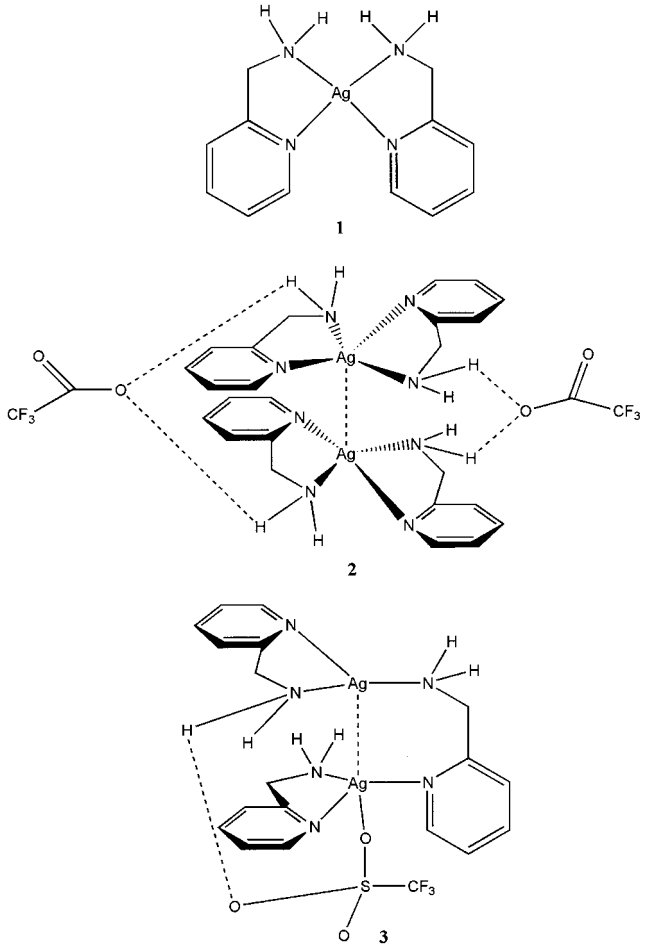

Scheme 1.

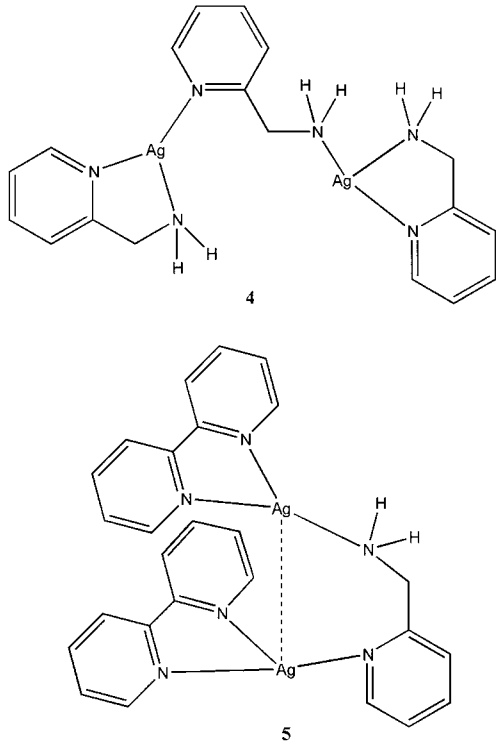

Scheme 2.

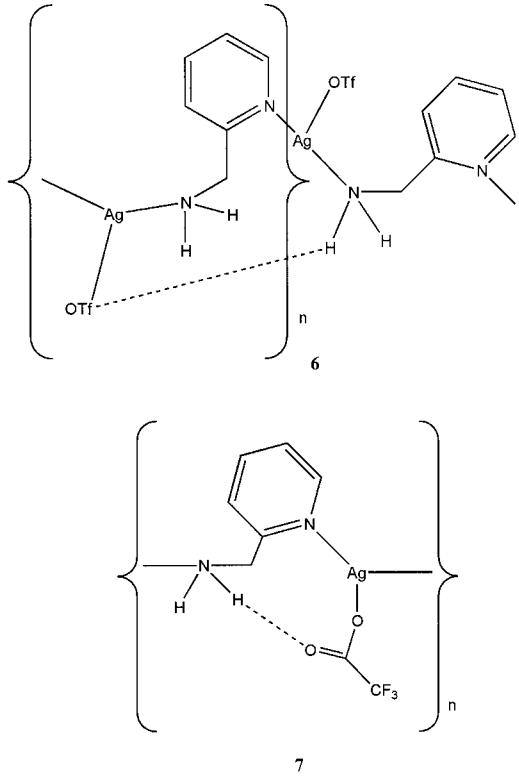

Scheme 3.

The ^1H NMR spectra of all the compounds are, as expected, generally similar. Signal shifts of the amine protons as well as of the *ortho*-*N*-hydrogen atoms on the pyridine rings are demonstrative of the differences in coordinated silver environments caused by the different anions present. The greatest shifts are seen examining the $–NH_2–$ protons in the presence of silver, ranging from 1.3 to 2.0 ppm downfield of the δ = 1.67 ppm chemical shift of the free 2-amp ligand in solution (NMR spectroscopic data for the free

ligand is available in the Supporting information; for Supporting information see also the footnote on the first page of this article). These shifts are implicative of solution-state complexation.

X-ray Crystallography

Structural confirmation of all the complexes mentioned herein was provided by X-ray diffraction studies. Single crystals of all compounds were analyzed and structural diagrams are displayed in Figures 2–10. A summary of the X-ray data is presented in Tables 1 and 2. Collections of selected bond lengths, angles, interatomic distances and hydrogen bonds are given in Tables 3, 4, and 5.

Description of the Crystal Structures

The ratio of 2-amp ligand/Ag in the structures of both compounds **1** and **2** is 2:1. A significant change in both the metal geometries and the ligand–metal bond lengths are seen when going from **1** to **2**, and are the result of differences in interaction of the BF_4^- and tfa^- anions. The structure of **2** contains a rather short Ag–Ag interaction[38] that is obtained at the expense of the relaxed tetrahedral environment of the metal-separated structure of **1**.

The expansion of the silver coordination environment from linear in a two-coordinate polymeric setting[23] to near tetrahedral upon the addition of 2 equiv. of the chelating 2-(aminomethyl)pyridine ligand to produce compound **1** was as expected. In the former structure, the only way to achieve the two-coordinate environment necessary to accommodate a 1:1 ratio of 2-amp/$AgBF_4$ is with an outward twisting of the ligand. In this way the amino and pyridine donors of separate 2-amp ligands are utilized, linking the linearly coordinated silver ions into a one-dimensional coordination polymer. In the latter, the increased coordination number allows for the formation of a chelated complex which is easily achieved by the 2-amp ligand creating the distorted tetrahedron that is shown in Figure 2. The deformation of the tetrahedral bond angles in this compound is caused by the small bite angle of the coordinated 2-amp ligands which averages 73°. The interligand angles are thus made more obtuse, ranging from 125.9(2)° to 133.9(2)°. BF_4^- ions are held in place in the lattice by H-bonding with the amine protons. The crystal structure of compound **1** contains two independent molecules of $(2\text{-amp})_2AgBF_4$ caused by slight differences in conformation. Amine–Ag and pyridine–Ag bonds cannot be distinguished from one another in this structure by bond lengths alone. Considerable overlap is seen with the amine–Ag distances ranging from 2.293(6) to 2.371(5) Å and the pyridine–Ag distances ranging from 2.262(6) to 2.368(4) Å.

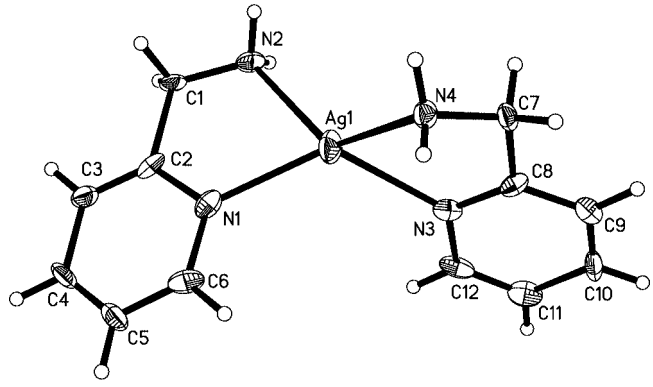

Figure 2. Molecular structure of one of the unique cationic monomers of **1**. Ellipsoids are drawn at the 50% probability level.

Table 1. Crystallographic data for compounds **1**–**4**.

	1	**2**	**3**	**4**
Empirical formula	$C_{24}H_{32}Ag_2B_2F_8N_8$	$C_{56}H_{64}Ag_4F_{12}N_{16}O_8$	$C_{20}H_{24}Ag_2F_6O_6S_2$	$C_{18}H_{24}Ag_2B_2F_8N_6$
Formula mass	821.94	1748.71	838.31	713.79
a [Å]	7.8817(5)	7.4205(6)	8.1167(9)	7.112(1)
b [Å]	14.0058(8)	13.284(1)	22.930(4)	8.335(2)
c [Å]	7.2894(4)	18.049(2)	15.625(2)	21.471(4)
α [°]	106.208(2)	69.342(4)		97.23(3)
β [°]	93.211(2)	89.255(4)	97.430(5)	98.51(3)
γ [°]	100.710(3)	80.621(4)		99.10(3)
V [Å^3]	754.25(8)	1640.8(2)	2883.7(7)	1228.4(4)
Z	1	1	4	2
Space group	$P\bar{1}$	$P\bar{1}$	$P2_{1/n}$	$P\bar{1}$
T [K]	110(2)	110(2)	110(2)	110(2)
$D_{calcd.}$ [g cm^{-3}]	1.810	1.770	1.931	1.930
μ [mm^{-1}]	1.379	1.275	1.588	1.675
$2\theta_{max.}$ [°]	28.31	26.43	28.30	28.39
Reflections measured	15414	54807	66994	14615
Reflections used (R_{int})	5828(0.0267)	12763(0.0401)	7095(0.0308)	5935(0.0226)
Restraints/parameters	7/391	3/865	0/397	10/341
R_1 [$I > 2\sigma(I)$]	0.0174	0.0274	0.0177	0.0274
wR_2 [$I > 2\sigma(I)$]	0.0465	0.0635	0.0432	0.0678
$R(F_o^2)$ (all data)	0.0184	0.0364	0.0226	0.0317
$R_w(F_o^2)$ (all data)	0.0472	0.0675	0.0443	0.0705
GOF on F^2	1.028	1.016	1.063	1.034

Table 2. Crystallographic data for compounds **5**–**7**.

	5	**6**	**7**
Empirical formula	$C_{26}H_{24}Ag_2B_2F_8N_6$	$C_7H_8AgF_3N_2O_3S$	$C_8H_8AgF_3N_2O_2$
Formula mass	809.87	365.08	329.03
a [Å]	10.5634(6)	12.982(6)	4.7270(8)
b [Å]	13.6804(9)	11.458(4)	9.898(2)
c [Å]	19.709(1)	7.709(5)	22.111(4)
α [°]			
β [°]		101.40(3)	
γ [°]			
V [Å^3]	2848.3(3)	1124(1)	1034.6(3)
Z	4	4	4
Space group	$P2_12_12_1$	$P2_{1/c}$	$P2_12_12_1$
T [K]	110(2)	110(2)	110(2)
$D_{calcd.}$ [g cm^{-3}]	1.889	2.157	2.112
μ [mm^{-1}]	1.457	2.017	1.978
$2\theta_{max}$ [°]	28.29	28.37	26.45
Reflections measured	33450	39350	13577
Reflections used (R_{int})	7004(0.0291)	2751(0.0310)	2121(0.0626)
Restraints/parameters	0/397	0/154	0/145
R_1 [$I > 2\sigma(I)$]	0.0174	0.0194	0.0200
wR_2 [$I > 2\sigma(I)$]	0.0408	0.0491	0.0443
$R(F_o^2)$ (all data)	0.0194	0.0232	0.0229
$Rw(F_o^2)$ (all data)	0.0412	0.0502	0.0450
GOF on F^2	1.067	1.067	1.067

Table 3. Selected bond lengths [Å], angles [°], and distances for the compounds $(2\text{-amp})_2AgBF_4$ (**1**) and $(2\text{-amp})_2Ag(tfa)$ (**2**).

1			
Ag1–N1	2.262(6)	Ag1–N3	2.319(5)
Ag1–N4	2.336(6)	Ag1–N2	2.371(5)
Ag2–N6	2.293(6)	Ag2–N7	2.310(5)
Ag2–N8	2.322(5)	Ag2–N5	2.368(4)
N1–Ag1–N3	125.6(2)	N1–Ag–1N4	131.9(2)
N3–Ag1–N4	72.5(2)	N1–Ag1–N2	74.61(2)
N3–Ag1–N2	133.9(2)	N4–Ag1–N2	128.3(2)
N6–Ag2–N7	133.4(2)	N6–Ag2–N8	126.5(2)
N7–Ag2–N8	74.4(2)	N6–Ag2–N5	73.3(2)
N7–Ag2–N5	125.9(2)	N8–Ag2–N5	133.3(2)
N2–H···F2[1]	3.123(7)	N6–H···F7[4]	3.146(6)
N2–H···F3[2]	3.068(6)	N6–H···F8[5]	3.031(6)
N4–H···F1[1]	3.049(6)	N8–H···F6[6]	3.070(7)
N4–H···F4[3]	3.101(6)	N8–H···F5[5]	3.090(7)
Symmetry transformations used to generate atoms: #1: $x-1, y, z+1$; #2: $x-1, y, z$; #3: $x, y, z+1$; #4: $x, y, z-1$; #5: $x+1, y, z-1$; #6: $x+1, y, z$.			
2			
Ag1–N2	2.309(3)	Ag1–N4	2.326(3)
Ag1–N3	2.402(3)	Ag1–N1	2.418(3)
Ag2–N–8	2.265(3)	Ag2–N6	2.273(3)
Ag2–N5	2.499(3)	Ag2–N7	2.558(3)
Ag3–N10	2.298(3)	Ag3–N12	2.339(3)
Ag3–N11	2.390(3)	Ag3–N9	2.425(3)
Ag4–N16	2.277(3)	Ag4–N14	2.292(3)
Ag4–N13	2.459(3)	Ag4–N15	2.516(3)
Ag1–Ag2	3.0077(4)	Ag3–Ag4	3.0305(4)
N2–Ag1–N4	146.3(1)	N2–Ag1–N3	119.4(1)
N4–Ag1–N3	71.5(1)	N2–Ag1–N1	72.6(1)
N4–Ag1–N1	113.8(1)	N3–Ag1–N1	151.7(1)
N2–Ag1–Ag2	105.64(8)	N4–Ag1–Ag2	107.98(7)
N3–Ag1–Ag2	76.79(7)	N1–Ag1–Ag2	75.17(7)
N8–Ag2–N6	174.6(1)	N8–Ag2–N5	112.8(1)
N6–Ag2–N5	72.5(1)	N8–Ag2–N7	71.7(1)
N6–Ag2–N7	106.1(1)	N5–Ag2–N7	124.9(1)
N8–Ag2–Ag1	91.69(8)	N6–Ag2–Ag1	84.96(8)
N5–Ag2–Ag1	116.92(7)	N7–Ag2–Ag1	117.73(7)
N10–Ag3–N12	147.3(1)	N10–Ag3–N11	118.9(1)
N12–Ag3–N11	71.2(1)	N10–Ag3–N9	73.5(1)
N12–Ag3–N9	113.5(1)	N11–Ag3–N9	151.3(1)
N10–Ag3–Ag4	108.08(8)	N12–Ag3–Ag4	104.59(7)
N11–Ag3–Ag4	73.78(7)	N9–Ag3–Ag4	77.76(7)
N16–Ag4–N14	176.1(1)	N16–Ag4–N13	110.8(1)
N14–Ag4–N13	72.7(1)	N16–Ag4–N15	72.7(1)
N14–Ag4–N15	107.0(1)	N13–Ag4–N15	124.3(1)
N16–Ag4–Ag3	90.13(8)	N14–Ag4–Ag3	86.76(8)
N13–Ag4–Ag3	113.12(7)	N15–Ag4–Ag3	122.55(7)
N2–H···O8[1]	2.993(4)	N10–H···O1	2.905(4)
N2–H···O5[2]	2.945(4)	N10–H···O3	2.988(4)
N4–H···N7[3]	3.380(4)	N12–H···O6	2.949(4)
N4–H···O2	3.087(4)	N12–H···N13[3]	3.144(4)
N6–H···O4[4]	2.965(4)	N14–H···O6	3.076(4)
N6–H···O2	3.060(4)	N14–H···O7[6]	2.974(4)
N8–H···O8[5]	2.965(4)	N16–H···O1	3.049(4)
N8–H···O5[2]	3.060(4)	N16–H···O3[4]	2.960(4)
Symmetry transformations used to generate atoms: #1: $x, y, z-1$; #2: $x, y+1, z-1$; #3: $x-1, y, z$; #4: $x+1, y, z$; #: 5 $x+1, y, z-1$; #6: $x+1, y-1, z$.			

The crystal structure of complex **2** is shown in Figure 3 and is demonstrative of the strong effects that hydrogen bonding and the exchange of anion can have upon the structural characteristics of these compounds. Stoichiometrically identical to **1**, the use of the strong H-bond-accepting trifluoroacetate results in an unexpected sandwiching of two of the cationic units that are present in **1**. The increased propensity of the trifluoroacetate ion to hydrogen bonds enables it to act as a bridge pulling two amine groups of what would be separate units into close proximity of one another. This bridging activity is seen to occur on both sides of a now dimetallic cluster utilizing all four amine groups. The result is that the metal centers are pulled into such proximity to one another as to form a significant metal–metal interaction at 3.0077(4) Å. Similar distances are

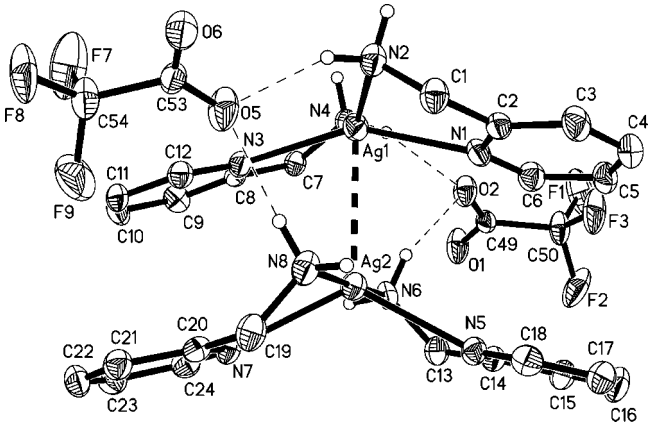

Figure 3. Molecular structure of one of the unique metal dimers of **2** showing how H-bonding to the anions hold the "sandwich" together. Ellipsoids are drawn at the 50% probability level. All hydrogen atoms except for those on the amine nitrogen atoms have been removed for clarity.

Table 4. Selected bond lengths [Å], angles [°], and distances for the compounds (2-amp)$_3$Ag$_2$(OTf)$_2$ (**3**), (2-amp)$_3$Ag$_2$(BF$_4$)$_2$ (**4**), and 2,2′-bpy$_2$(2-amp)Ag$_2$(BF$_4$)$_2$ (**5**).

3			
Ag1–N3	2.211(1)	Ag1–N2	2.277(1)
Ag1–N1	2.396(1)	Ag1–O1	2.591(1)
Ag2–N4	2.199(1)	Ag2–N6	2.236(1)
Ag2–N5	2.403(1)	Ag1–Ag2	2.9137(3)
N3–Ag1–N2	159.77(4)	N3–Ag1–N1	122.35(4)
N2–Ag1–N1	73.09(4)	N3–Ag1–O1	88.42(4)
N2–Ag1–O1	96.65(4)	N1–Ag1–O1	114.76(4)
N3–Ag1–Ag2	74.26(3)	N2–Ag1–Ag2	85.69(3)
N1–Ag1–Ag2	130.76(3)	O1–Ag1–Ag2	111.41(2)
N4–Ag2–N6	165.33(5)	N4–Ag2–N5	119.63(4)
N6–Ag2–N5	74.73(4)	N4–Ag2–Ag1	80.05(4)
N6–Ag2–Ag1	91.03(3)	N5–Ag2–Ag1	115.98(3)
N2–H···O2^1	3.1438(17)	N4–H···O4	2.9911(17)
N2–H···O6^2	3.1422(17)	N6–H···O2	3.0426(18)
N4–H···O5^2	2.9799(17)	N6–H···O3^1	3.0810(18)

Symmetry transformations used to generate atoms: #1: $-x + 1, -y, -z$; #2: $-x + 1, -y, -z + 1$.

4			
Ag1–N3	2.185(2)	Ag1–N2	2.267(2)
Ag1–N1	2.355(2)	Ag2–N4	2.186(2)
Ag2–N6	2.287(2)	Ag2–N5	2.313(2)
Ag1–Ag2	5.794(2)		
N3–Ag1–N2	154.73(8)	N3–Ag1–N1	130.16(7)
N2–Ag1–N1	74.86(8)	N4–Ag2–N6	146.26(8)
N4–Ag2–N5	135.55(7)	N6–Ag2–N5	74.97(7)
N2–H···F8A^1	3.055(16)	N4–H···F4	3.112(3)
N2–H···F5^1	3.094(3)	N4–H···F1^1	2.982(3)
N2–H···F8^1	3.330(4)	N6–H···F4^2	3.133(3)
N2–H···F7A	2.97(3)	N6–H···F1^2	3.384(3)
N2–H···F7	3.211(5)	N6–H···F2	3.000(3)

Symmetry transformations used to generate atoms: #1: $x + 1, y, z$; #2: $-x + 2, -y, -z + 1$.

5			
Ag1–N1	2.150(2)	Ag1–N3	2.270(1)
Ag1–N4	2.284(2)	Ag2–N2	2.178(2)
Ag2–N6	2.287(2)	Ag2–N5	2.329(2)
Ag1–Ag2	2.8958(3)		
N1–Ag1–N3	136.91(6)	N1–Ag1–N4	148.32(6)
N3–Ag1–N4	73.34(5)	N1–Ag1–Ag2	82.92(4)
N3–Ag1–Ag2	100.56(4)	N4–Ag1–Ag2	81.52(4)
N2–Ag2–N6	142.97(6)	N2–Ag2–N5	145.38(6)
N6–Ag2–N5	71.65(5)	N2–Ag2–Ag1	86.46(4)
N6–Ag2–Ag1	85.99(4)	N5–Ag2–Ag1	99.82(4)
N2–H···F5^1	2.977(2)	N2–H···F2^1	3.1257(19)
N2–H···F3^1	3.099(2)		

Symmetry transformations used to generate atoms: #1: $x, y + 1, z$.

Table 5. Selected bond lengths [Å], angles [°], and distances for the compounds (2-amp)AgOTf (**6**) and (2-amp)Ag(tfa) (**7**).

6			
Ag1–N2^1	2.144(2)	Ag1–N1	2.145(2)
Ag1–O2	2.644(2)	Ag1–Ag1^2	5.977(2)
N2^1–Ag1–N1	171.93(6)		
N2–H···O1^3	2.913(2)	N2–H···O1^5	2.993(3)
N2–H···O3^4	2.967(3)		

Symmetry transformations used to generate atoms: #1: $-x + 2, y + 1/2, -z + 1/2$; #2: $-x + 2, y - 1/2, -z + 1/2$; #3: $-x + 1, y - 1/2, -z + 1/2$; #4: $-x + 1, -y + 1, -z$; #5: $-x + 1, -y + 1, -z + 1$.

7			
Ag1–N2^1	2.186(2)	Ag1–N1	2.188(2)
Ag1–O1	2.498(2)	Ag1–Ag1^2	5.437(1)
N2^1–Ag1–N1	152.96(9)	N2^1–Ag1–O1	94.27(8)
N1–Ag1–O1	110.63(8)		
N2–H···O2	2.922(3)	N2–H···O1^3	2.904(3)

Symmetry transformations used to generate atoms: #1: $-x + 1, y + 1/2, -z + 1/2$; #2: $-x + 1, y - 1/2, -z + 1/2$; #3: $-x + 2, y - 1/2, -z + 1/2$.

normally found only in complexes where the interacting silver ions are being bridged directly by another donor or anion.[27] This is a noteworthy interaction seeing as how the tetrahedral environments of the individual metal centers have to undergo considerable distortions in order to achieve a geometry that allows for the contact to occur. The resulting metal–metal interaction hence seems not only to be lightly supported, but even unfavored. The reasoning behind the fact that the complex does not snap apart to become isostructural with **1** lies in the fact that the silver(I) ion is extremely flexible in its coordination sphere. In order to accommodate the silver–silver interaction the two metal centers must contort into two quite different conformations. The top silver ion adopts a distorted square-based pyramidal arrangement. For this to occur the N–Ag bond lengths are stretched to suit the new setting with the pyridine–silver bonds being stretched more, making it now possible to distinguish between the two types of donors on the basis of bond lengths. Amine–silver lengths range from 2.298(3) to 2.339(3) Å whereas the pyridine–silver lengths are stretched slightly longer to between 2.390(3) and 2.425(3) Å. The bottom silver ion suffers a similar contortion that leaves it in a trigonal-bipyramidal setting with both amine groups occupying the axial positions. Pyridine donors and the metal–metal interaction hold the equatorial spaces. This distinct difference in coordination sites assists in broadening the division between the lengths of the amine– and pyridine–silver separations; the axial amine–silver distances range from 2.265(3) to 2.292(3) Å while the equatorial pyridine–silver distances range from 2.459(3) to 2.558(3) Å. Looking outward from the initial interdimeric H-bonded bridge it is noticed that each oxygen atom of the trifluoroacetate ion is used to hold a separate set of these stacked complexes on top of each other such that the anion acts in an η^2,μ_4-fashion. This effectively constructs a linear chain of dimetallic clusters held together by hydrogen bonds.

The molecular structures of compounds **3** and **4** offer another example of the marked effect that changes in the H-bond-accepting ability of the anion has upon the conformation of the molecule. Ratios of ligand/metal in both complexes are 3:2 such that the structural differences again are being caused solely by the anion. The addition of a more strongly interacting anion has the effect of closing the 3:2 structure onto itself.

In **3**, the ratio of ligand/metal is controlled, or at least limited, by the anion. It is seen that even a fivefold excess of 2-amp does not force a ratio higher than 3:2 in the crystal structure shown in Figure 4. This is accredited to a bifunctional role of the triflate ion in the complex: its first function is to act as a coordinating anion to one of the

metal ions, and its second is to concomitantly engage in an intramolecular H-bond through a separate oxygen atom. The addition of more than 1 equiv. of 2-amp disrupts the linear coordination environment that the silver ion has when the ligand is present in only 1 equiv. (as in compound **6**). The first 0.5 equiv. of ligand that is added past an initial 1:1 ratio forms a bridge joining two 2-amp-chelated silver(I) units. After this point, a triflate ion that binds to one of the metal centers through a single oxygen atom halts the addition of a full second equivalent of 2-amp ligand to the silver ions. In this orientation the triflate ion is then able to H-bond through a second oxygen atom to the amine protons of the ligand chelating the opposite silver ion. The effect is similar to that seen in compound **2**; H-bonding with the anion holds the silver ion bound only to nitrogen atoms sufficiently close to the anion-bound silver ion to create a strong metal–metal interaction. However, the geometry of the SO_3 portion of the triflate allows it to be involved in both coordination and H-bonding, thus forcing the structural difference with **2**. The bridging 2-amp ligand acts as a hinge as the H-bonded anion squeezes the silver ions to within 2.9137(3) Å of one another. In this structure there is a notable difference in bond lengths between the two types of ligands present. This should be expected as the stress of the five-membered ring is relieved in going from a chelating to a more relaxed bridging six-membered system. The chelated amine–silver distances are 2.277(1) and 2.236(1) Å and the chelated pyridine–silver distances are 2.396(1) and 2.403(1) Å. The same distances measured for the bridging ligand are noticeably shorter at 2.199(1) and 2.211(1) Å, respectively. The coordinating O1 atom has a bond length to Ag1 of 2.590(1) Å. In this structure, as in the last two, intermolecular H-bonding again plays a role in determining the packing of the complex with another 1-D "polymer" being constructed of the dimetallic units held together by H-bonds to the anions. H-bonds to O2 and O3 fashion a sort of dimer, while those to the non-coordinating anions assemble these dimers into a chain.

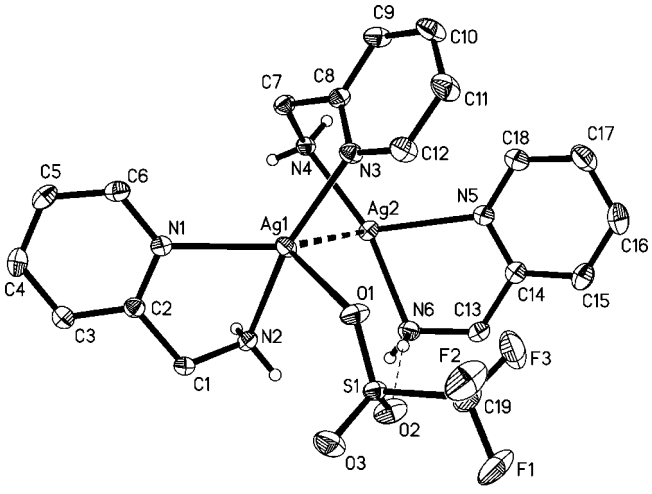

Figure 4. Molecular structure of the monopositive cation in **3**. Ellipsoids are drawn at the 50% probability level. All hydrogen atoms except for those on the amine nitrogen atoms have been removed for clarity.

In the absence of an anion capable of strongly receiving an H-bond the cationic closed structure of compound **3** opens to form the flat 3:2 complex **4**. The structure, as shown in Figure 5, is an intermediate one that bridges the gap between the polymer formed by 2-amp and $AgBF_4$ in the 1:1 ratio and the discrete structure of compound **1** with its 2:1 ratio, making $AgBF_4$ the only silver salt studied with which all three of these ratios were able to be achieved. Without the H-bonding of the anion to hold them together, the metal centers situate themselves widely separated by 5.794(2) Å on opposite sides of the bridging ligand. Each silver ion is then chelated by another 2-amp ligand creating a nearly planar dimetallic complex. Although twists and rotations about the center bridging ligand are likely to be occurring in solution, stacking of the molecules into sheets, as well as π–π interactions help keep them flat in the solid state. The distance between the planes of the aromatic rings averages around 3.2 Å from one layer to the next in the crystal structure. The BF_4^- anions can be seen to fit nicely into holes formed by this stacking of molecules and are held in place by weak H-bonds to the amine nitrogen atoms. The chelating amine–silver distances in **4** are 2.267(2) and 2.287(2) Å and the pyridine–silver distances are 2.313(2) and 2.355(2) Å. The bridging amine–silver and pyridine–silver distances are again seen to be quite shorter at 2.186(2) and 2.185(2) Å. Angles around the silver ions are distorted from the ideal 120° trigonal geometry due to the small bite angle of the chelating 2-amp ligand and have values ranging from 74.97(7) to 154.73(8)°. However, deviations of the silver ions from their respective three-nitrogen planes are small at 0.054(1) Å for Ag1 and 0.170(1) Å for Ag2, showing that they are still very much in a planar environment.

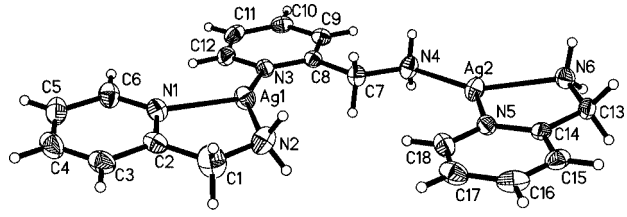

Figure 5. View of the cationic complex of **4**. Ellipsoids are drawn at the 50% probability level.

Compound **5** was prepared in an attempt to mimic the structural characteristics of **4** using 2,2′-bipyridine as the chelating ligand that caps the ends of the dimetallic structure. The addition of 2 equiv. of 2,2′-bipyridine to a solution that is 1:2 in 2-amp/$AgBF_4$ does indeed produce a compound that is stoichiometrically identical to **4** (when the bipyridine is substituted for the chelating 2-amp ligands). However, what resulted was the unexpected hybrid shown in Figure 6 that contains features of both **3** and **4**. The 2-amp ligand acts as expected in the presence of an excess of $AgBF_4$, bridging two separate metal centers. The addition of 2,2′-bipyridine results in two 2,2′-bipyridine-chelated silver ions separated by the bridging 2-amp ligand.

The connectivity of the structure formed is analogous to that seen in **4**. Otherwise, the similarities between this and **4** are few. Instead of opening up to make a flat structure, the amine-bound silver ion twists back around to form an interaction with the pyridine-bound silver ion. The resulting hairpin structure bears closer resemblance to the triflate salt in **3**. A major difference here is that there are no good H-bond donors on the bipyridine ligands and no strongly H-bond-accepting anion to link the chelating ligands, as in **2** and **3**. This leaves only the weaker π-stacking forces of the two bipyridine ligands to account for the conformation of this compound. The angle of the bipyridine planes from one another is a rather obtuse 28.4° and the ring centers are separated by an average of 4.546 Å. This lends itself to the observation that the argentophilic interaction in these compounds is a highly favored one and the 2-amp ligand bridging two interacting silver ions appears to be only slightly higher in energy than the conformation in which the silver ions are completely separated. There is also fairly prominent intermolecular π-stacking of the bipyridine rings both above and below each molecule with the parallel ring planes averaging only 3.316 Å from one another. The N–Ag distances here are quite short, second only to those seen in the polymer complex **6**. The Ag1–pyridine bond length is 2.150(2) Å and the Ag2–amine distance is 2.178(2) Å. The bipyridine-N–Ag distances are more along the lines of the lengths that have been displayed so far and range from 2.271(1) to 2.330(2) Å.

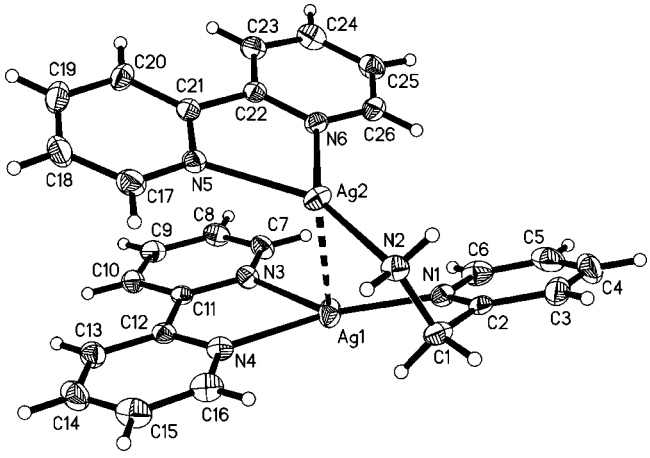

Figure 6. View of the cationic complex of **5**. Ellipsoids are drawn at the 50% probability level.

Compounds **6** and **7** show the result of the addition of the 2-amp ligand to silver triflate and trifluoroacetate salts in a 1:1 ratio. In the absence of a sufficient amount of strong donor sites to construct at least a three-coordinate environment around the metal center (in this case N-donors), each silver ion attempts to adopt its desired linear coordination environment. Since a maximum bite angle of around only 75° is obtainable with the chelating 2-amp ligand, donors from two separate ligands must be used in order to achieve this arrangement. The results are linear zigzag coordination polymers similar to those seen previously with noncoordinating anions.[23] In the case of **6** and **7**, the anions display an increasing coordination ability resulting in varying degrees of perturbation of the metal centers from their ideal linear geometry. They also allow for H-bonding within the polymer and to adjacent polymers, adding to the dimensionality of the structure.

2-(Aminomethyl)pyridine together with 1 equiv. of silver triflate assembles into a zigzagging 1-dimensional coordination polymer containing silver ions with a T-shape geometry, compound **6**. The unique portion of the polymer, shown in Figure 7, contains one silver ion bound in near-linear coordination by an amine nitrogen atom and its symmetry-equivalent pyridine nitrogen atom. The triflate anion is coordinated as well through a stretched bond to O1. When perpetuated, the 2-(aminomethyl)pyridine backbone of the polymer, shown in Figure 8, is seen to be nearly planar both perpendicular to and in the direction of its growth. This is similar to the conformation displayed in compound **4** and is likely the result of a combination of ring stacking and hydrogen bonding. The linear chains are stacked one on top of another with each row slightly offset from the previous as to accommodate the anions protruding into the next layer. The layers are held together throughout the length of the polymers by the interpolymeric hydrogen bonding of each triflate ion to an amine group both above and below the plane in which it is in. The triflate ions are held in the plane of the polymer by intrapolymeric H-bonding to an amine in the next unit. This also likely assists in keeping the planarity of the polymer. The triflate-O–Ag bond is a weak one at 2.644 Å, which is apparent from the only slight bending of the amine–Ag–pyridyl angle of

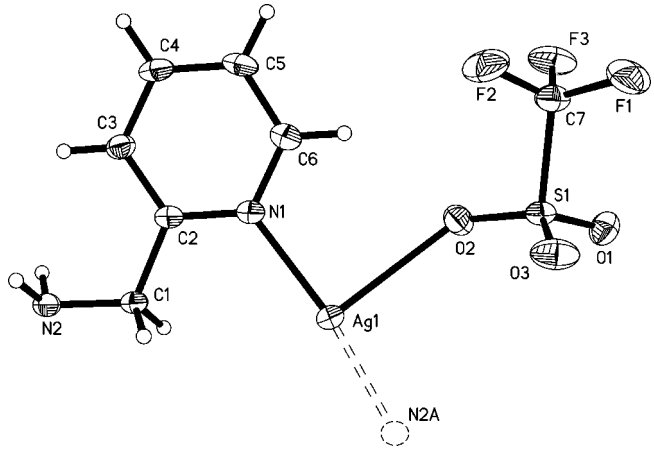

Figure 7. View of the unique portion of the polymer of **6** with the coordination environment about the silver ion shown complete. Ellipsoids are drawn at the 50% probability level.

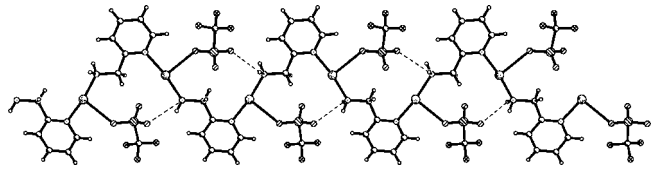

Figure 8. View of the 1-D polymer of **6** showing the intrapolymeric H-bonding.

171.93(6)°. The N–Ag distances of this polymer are the shortest displayed herein at 2.145(2) Å for the pyridine–Ag length and 2.144(2) Å for the amine–silver distance.

The unique portion of compound **7**, shown in Figure 9, again contains a single silver ion, 2-amp ligand, and anion. It is made apparent here that trifluoroacetate acts as a stronger coordinating anion than triflate when there are insufficient N-donors to saturate the coordination sites of the silver ion. The 1-dimensional coordination polymer backbone of **7** that is seen in Figure 10 is connectively very similar to that of **6**. The more strongly interacting anion, while generally occupying the same spaces in the polymer as those held by triflate in the previous structure, imparts structural features not formerly seen. O1 coordinates strongly to Ag with a bond length of 2.498(2) Å, distorting the pyridine–Ag–amine angle to 152.96(9)°. This distortion causes the amino nitrogen atom to be pushed out of its planar position to give the linear polymer an overall helical appearance seen looking down the length of the polymer. With its remaining oxygen atom, the trifluoroacetate ion extends a bridge both above and, by symmetry equivalence, below the original polymer to link to silver ions of adjacent polymers. This stretched interaction at 2.715(2) Å crosslinks the helical polymers into a pseudo-2-dimensional pleated sheet structure. The intrapolymeric H-bonding here serves to help hold the 1-dimensional polymer into its spiraling conformation. The N–Ag bond lengths are quite short in this polymer as they were in compound **6**, though the presence of the more strongly donating anion causes them to lengthen slightly. The pyridine–Ag distance is 2.188(2) Å and the amine–Ag distance is 2.186(2) Å.

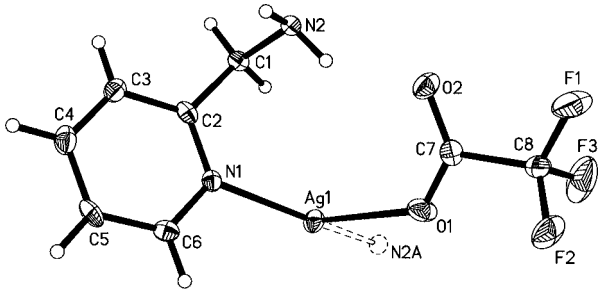

Figure 9. Molecular diagram of the unique portion of **7** with the coordination environment about the silver ion shown complete. Ellipsoids are drawn at the 50% probability level.

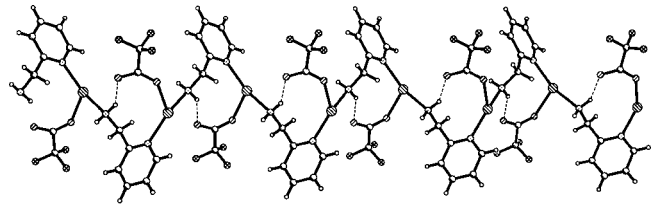

Figure 10. View of the helical 1-D polymer formed by compound **7** showing the intrapolymeric H-bonding.

Luminescence Properties

Interest in hybrid inorganic–organic polymers for application as potential new "organic" light-emitting devices (OLEDs) has been on a steady rise over the past decade. Their versatility comes from the ability to tune their absorption and emission spectra by (typically) facile modifications to the metal environment. Such tuning is not an easy option for the strictly organic LEDs, which often require drastic synthesis and modifications to alter their photoluminescent properties.[42] All excitation and emission spectra were recorded at concentrations of 1×10^{-4} M in acetonitrile glasses at 77 K. The low-temperature solution luminescence was collected to give a general representation of what the solid-state excitation and emission would be, given that in the 77 K glasses there is substantial complex character (polymeric character in the case of compounds **6** and **7**).[18,43,44] Luminescence spectra of representative compounds are displayed in Figure 11. A more complete collection of spectra are available in the supporting information.

Discussion of Luminescence

The resemblance of the excitation spectra of compounds **1**–**7** with that of the free 2-(aminomethyl)pyridine ligand suggests that the luminescent behavior of these complexes is initiated by a ligand-based absorption, which then decays by means of ligand-to-metal charge transfer. Excitation maxima of all compounds are presented in

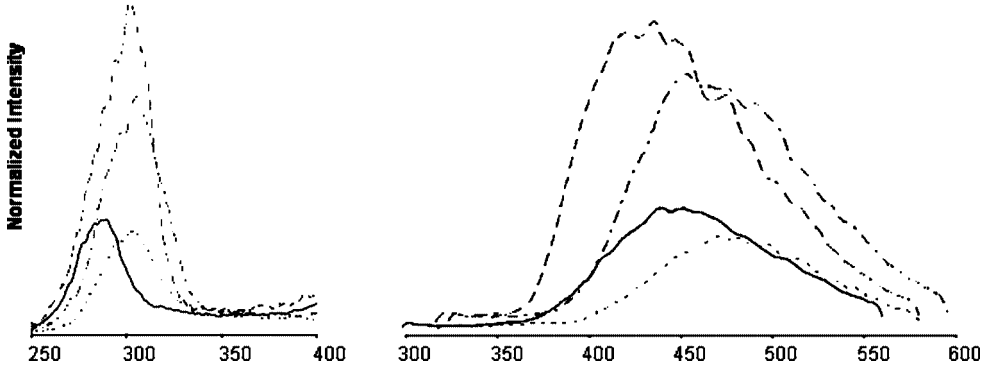

Figure 11. Normalized excitation and emission spectra of compounds **1**, **3**, **6**, and **7** taken in acetonitrile glasses at 1×10^{-4} M concentration at 77 K. —— = (2-amp)AgOTf, – – – = (2-amp)Ag(tfa), ····· = $(2\text{-amp})_2AgBF_4$, –·–·– = $Ag_2(2\text{-amp})_3(OTf)_2$.

Table 6 along with the local emission maxima. The emission spectra of the various compounds cover a modest range of the spectrum with local maxima spanning approximately 100 nm. The strongest emissions are seen to be produced by the compounds that have the most interacting anions, OTf and tfa, and of these the coordination polymer **7**, likely accredited to the extended networks of electronic interaction, shows a stronger emission. It is seen that the most intense luminescence, that of the 1:1 (2-amp)Ag(tfa) polymer, also occurs at the most energetic wavelengths with three strong transitions at 422, 436, and 448 nm. As a general trend, as the intensity of the luminescence drops off, so does the energy of the transitions. The next most intense emission comes from the 3:2 (2-amp)AgOTf cluster **3** with its strongest maxima at 453 nm, followed by the silver "sandwich" complex **2** at 460 nm. The triflate polymer **6** and the tetrafluoroborate monomers of **1** show similar intensity with maxima at 441 and 473 nm, respectively.

Table 6. Luminescent spectral data for compounds **1**–**7** at 77 K and 1×10^{-4} M in CH_3CN.

Compound	Excitation λ_{max} [nm]	Emission local λ_{min} [nm]
2-amp	318	378
1	303	472, 483, 500, 516
2	303	460, 470, 495
3	307	454, 468, 477, 492
4	300	446, 454, 462, 475
5	369	392, 435
6	290	440, 452, 462
7	302	422, 437, 449, 476

Conclusions

We have demonstrated here that a variety of silver(I) complexes can be formed with the bidentate nitrogen ligand 2-(aminomethyl)pyridine. The complexes, their structures and luminescent characteristics are seen to be highly dependent not only on the hydrogen-bonding and coordinating ability of the anion but also on the ratio of ligand/metal. The simplicity of the 2-amp ligand made it a desirable prospect for this concentration/counterion study that produced molecular structures ranging from simple monomers to folded dimetallic metal–metal interacting species to elaborate multidimensional polymers. This same type of behavior is currently being investigated in the 3- and 4-(aminomethyl)pyridines which have demonstrated great potential for the formation of coordination polymers and macromolecules by removing the ability to chelate that has been so prevalent in the 2-amp structures. Results of these studies will form the basis of further publications.

Experimental Section

General Remarks: All experiments were carried out under argon using a Schlenk line and standard Schlenk techniques. Glassware was dried at 120 °C for several hours prior to use. All reagents except 2,2′-bipyridine, which was stored in a bench top dessicator, were stored in a glovebox with an inert gas. Acetonitrile and diethyl ether were distilled from calcium hydride and sodium/benzophenone ketyl, respectively, immediately before use. 2-(Aminomethyl)-pyridine and 2,2′-bipyridine were purchased from Aldrich and used as received. Silver(I) trifluoroacetate, silver(I) trifluoromethanesulfonate, and silver(I) tetrafluoroborate were purchased from Strem Chemicals Inc. and used as received. ^{1}H NMR spectra were recorded at 300.13 MHz with a Bruker Spectrospin 300 MHz spectrometer. Elemental analyses were performed by Atlantic Microlabs Inc. in Norcross, Georgia. Excitation and emission spectra were recorded with an Instruments S. A. Inc. Fluoromax-2 model spectrometer using band pathways of 5 nm for both excitation and emission and are presented uncorrected.

General Synthesis: General procedures for the synthesis of compounds **1**–**4**, **6**, and **7** involved the addition of an acetonitrile solution (5 mL) of 2-(aminomethyl)pyridine to a stirred solution of the appropriate silver salt in acetonitrile (5 mL). The mixtures were stirred for 10 min then dried in vacuo to leave white to off-white powders. All flasks were shielded from light with aluminum foil to prevent the photodecomposition of the silver compounds. Crystals of compound **2** were grown by slow diffusion of hexanes into a dichloromethane solution at 5 °C. Crystals of compound **5** were grown by slow diffusion of diethyl ether into a dichloromethane solution at 5 °C. Crystals of all other compounds were obtained by slow diffusion of diethyl ether into acetonitrile solutions at 5 °C. The amount of reagents used, yields, and analytical data are presented in the following paragraphs as well as any modifications to the general synthetic procedure. Yields are based on the amount of silver salt used.

Synthesis of $Ag(2\text{-amp})_2BF_4$ (1): This reaction used 2 equiv. of 2-(aminomethyl)pyridine (0.111 g, 1.03 mmol) added to $AgBF_4$ (0.100 g, 0.51 mmol) to leave a white flaky solid in 92% (0.19 g, 0.47 mmol) yield upon solvent evaporation. Colorless block-shaped crystals were formed. ^{1}H NMR (298 K, CD_3CN): δ = 2.93 (br. s, 4 H, NH_2), 4.14 (s, 4 H, CH_2), 7.28 (m, 2 H), 7.739 (td, J_{H-Ho} = 7.5, J_{H-Hm} = 1.5 Hz, 4 H), 8.49 (d, J_{H-Ho} = 6.0 Hz, 2 H) ppm. $AgC_{12}H_{16}N_4BF_4$ (410.95): calcd. C 35.07, H 3.92, N 13.63; found C 35.03, H 3.78, N 13.33.

Synthesis of $Ag(2\text{-amp})_2(tfa)$ (2): This reaction used 2 equiv. of 2-(aminomethyl)pyridine (0.098 g, 0.91 mmol) added to Ag(tfa) (0.100 g, 0.45 mmol) to leave a light-brown fluffy solid in 82% (0.16 g, 0.37 mmol) yield upon evaporation of the solvent. Colorless block-shaped crystals were formed. ^{1}H NMR (298 K, CD_3CN): δ = 3.47 (br. s, 4 H, NH_2), 3.83 (s, 4 H, CH_2), 7.29 (m, 2 H), 7.77 (d, J_{H-Ho} = 6.0 Hz, 4 H), 8.48 (s, 2 H) ppm. $AgC_{14}H_{16}N_4O_2F_3$ (437.17): calcd. C 38.46, H 3.69, N 12.82; found C 38.24, H 3.57, N 12.54.

Synthesis of $Ag_2(2\text{-amp})_3(OTf)_2$ (3): This reaction used 3 equiv. of 2-(aminomethyl)pyridine (0.063 g, 0.58 mmol) added to 2 equiv. of AgOTf (0.100 g, 0.39 mmol). An oily yellow solid was left upon evaporation of the solvent in vacuo. This was then redissolved in a small amount of CH_3CN and precipitated with ether to leave a fluffy white solid in 76% (0.12 g, 0.15 mmol) yield upon drying. Colorless block-shaped crystals were formed. ^{1}H NMR (298 K, CD_3CN): δ = 3.32 (br. s, 6 H, NH_2), 4.11 (s, 6 H, CH_2), 7.28 (m, 3 H), 7.74 (td, J_{H-Ho} = 7.5, J_{H-Hm} = 1.5 Hz, 6 H), 8.49 (d, J_{H-Ho} = 6.0 Hz, 3 H) ppm. $Ag_2C_{20}H_{24}N_6O_6F_6S_2$ (838.31): calcd. C 28.86, H 2.89, N 10.02; found C 29.29, H 2.92, N 10.00.

Synthesis of $Ag_2(2\text{-amp})_3(BF_4)_2$ (4): This reaction used 3 equiv. of 2-(aminomethyl)pyridine (0.150 g, 1.39 mmol) added to 2 equiv. of $AgBF_4$ (0.180 g, 0.92 mmol). A white powder was left in 84% yield (0.278 g, 0.39 mmol) upon evaporation of the solvent in vacuo.

Colorless block-shaped crystals were formed. ^{1}H NMR (298 K, CD_3CN): δ = 3.12 (br. s, 6 H, NH_2), 4.15 (s, 6 H, CH_2), 7.29 (m, 3 H), 7.75 (td, $J_{H–Ho}$ = 7.4, $J_{H–Hm}$ = 1.5 Hz, 6 H), 8.50 (s, 3 H) ppm.

Synthesis of $Ag_2$2,2′-bpy$_2$(2-amp)$(BF_4)_2$ (5): This reaction used 2-(aminomethyl)pyridine (0.050 g, 0.46 mmol) added to 2 equiv. of $AgBF_4$ (0.180 g, 0.93 mmol). This solution was stirred for 10 min, then 2 equiv. of 2,2′-bipyridine (0.144 g, 0.92 mmol) in 5 mL of CH_3CN was added. This was stirred an additional 5 min, then dried in vacuo to leave an off-white powder in 90% (0.126 g, 0.22 mmol) yield. Colorless block-shaped crystals were formed. ^{1}H NMR (298 K, CD_3CN): δ = 3.19 (br. s, 2 H, NH_2), 4.05 (s, 2 H, CH_2), 7.43 (m, 8 H), 7.89 (m, 9 H), 7.98 (d, $J_{H–Ho}$ = 8.1 Hz, 2 H), 8.36 (d, $J_{H–Ho}$ = 4.8 Hz, 1 H) ppm.

Synthesis of Ag(2-amp)OTf (6): This reaction used 2-(aminomethyl)-pyridine (0.042 g, 0.39 mmol) added to AgOTf (0.100 g, 0.39 mmol) to leave an oily brown solid upon evaporation of the solvent. This solid was then redissolved in a small amount of CH_3CN and precipitated with diethyl ether to leave a brown solid in 85% (0.120 g, 0.33 mmol) yield. Colorless block-shaped crystals were formed. ^{1}H NMR (298 K, CD_3CN): δ = 3.42 (br. s, 2 H, NH_2), 4.16 (s, 2 H, CH_2), 7.25 (m, 1 H), 7.77 (td, $J_{H–Ho}$ = 6.9, $J_{H–Hm}$ = 1.0 Hz, 2 H), 8.52 (d, $J_{H–Ho}$ = 3.6 Hz, 1 H) ppm. $AgC_7H_8N_2O_3SF_3$ (365.08): calcd. C 25.80, H 2.47, N 8.56; found C 26.27, H 2.33, N 8.77.

Synthesis of Ag(2-amp)(tfa) (7): This reaction used 2-(aminomethyl)-pyridine (0.049 g, 0.45 mmol) added to Ag(tfa) (0.100 g, 0.45 mmol) to leave an off-white powder in 75% (0.11 g, 0.34 mmol) yield upon evaporation of the solvent. Colorless plates were formed. ^{1}H NMR (298 K, CD_3CN): δ = 3.68 (s, 2 H, NH_2), 4.11 (s, 2 H, CH_2), 7.28 (m, 1 H); 7.75 (td, $J_{H–Ho}$ = 7.5, $J_{H–Hm}$ = 1.5 Hz, 2 H), 8.53 (d, $J_{H–Ho}$ = 6.0 Hz, 1 H) ppm. $AgC_8H_8N_2O_2F_3$ (329.03): calcd. C 29.20, H 2.45, N 8.51; found C 29.38, H 2.39, N 8.40.

X-ray Crystallographic Study: Crystallographic data were collected on crystals with dimensions 0.181 × 0.150 × 0.100 mm for **1**, 0.210 × 0.150 × 0.090 mm for **2**, 0.279 × 0.216 × 0.202 mm for **3**, 0.310 × 0.270 × 0.250 mm for **4**, 0.245 × 0.231 × 0.199 mm for **5**, 0.167 × 0.143 × 0.094 mm for **6**, and 0.240 × 0.150 × 0.080 mm for **7**. Crystals of all compounds were immobilized on a cryoloop by encasing them in Paratone-N oil then cooling them in a nitrogen cold stream. Data were collected at 110 K with a Bruker X8 Apex. Graphite-monochromated Mo-K_α radiation (λ = 0.71073 Å) was used throughout. All structures were solved by direct methods after processing with SAINT-Plus and correction of the data using SADABS.[45] All of the data were processed with the Bruker AXS SHELXTL software, version 6.10.[43] All non-hydrogen atoms were refined anisotropically and hydrogen atoms were placed in calculated positions except for the amine hydrogen atoms of compound **3**, whose positions were allowed to refine. The crystal structures of compounds **1** and **2** each contain 2 unique monomers of their respective compounds. The structure of compound **4** contains a BF_4^- anion disordered over 2 positions. The anisotropic displacement parameters for the two orientations of the disorder are constrained to be equal and the site occupancies were refined as 0.825(3)/0.173(3) [for B(1/1a), F(1/1a), F(2/2a), F(3/3a), F(4/4a)]. CCDC-260748 (**1**), -260750 (**2**), -260753 (**3**), -262119 (**4**), -260752 (**5**), -260751 (**6**), and -260749 (**7**) contain the supplementary crystallographic data for this paper. These data can be obtained free of charge from The Cambridge Crystallographic Data Centre via www.ccdc.cam.ac.uk/data_request/cif.

Supporting Information (see footnote on the first page of this article): Additional figures showing extended H-bonding networks, stacking, and 3-D growth of compounds **2**, **6**, and **7** are available as well as full excitation and emission spectra for all compounds reported.

Acknowledgments

This research was supported by funds provided by grant from the Robert A. Welch Foundation (AA-1508). The Bruker X8 APEX diffractometer was purchased with funds received from the National Science Foundation Major Research Instrumentation Program Grant CHE-0321214.

[1] J. Y. Lu, *Coord. Chem. Rev.* **2003**, *246*, 327–347.
[2] C. Janiak, *J. Chem. Soc., Dalton Trans.* **2003**, 2781–2804.
[3] Y.-B. Xie, J.-R. Li, X.-H. Bu, *Polyhedron* **2005**, *24*, 413–418.
[4] J. T. Sampanthar, J. J. Vittal, *Cryst. Eng.* **2000**, *3*, 117–133.
[5] Z.-L. You, H.-L. Zhu, W.-S. Liu, *Acta Crystallogr., Sect. C* **2004**, *60*, m620–m622.
[6] R. P. Feazell, C. E. Carson, K. K. Klausmeyer, *Acta Crystallogr., Sect. C* **2004**, *60*, m598–m600.
[7] M. A. S. Goher, A. K. Hafez, M. A. M. Abu-Youssef, A. M. A. Badr, C. Gspan, F. A. Mautner, *Polyhedron* **2004**, *23*, 2349–2356.
[8] Y.-B. Dong, X. Zhao, R.-Q. Huang, M. D. Smith, H.-C. z. Loye, *Inorg. Chem.* **2004**, *43*, 5603–5612.
[9] D. J. Eisler, R. J. Puddephatt, *Cryst. Growth Des.* **2005**, *5*, 57–59.
[10] A. L. Pickering, D.-L. Long, L. Cronin, *Inorg. Chem.* **2004**, *43*, 4953–4961.
[11] M. Vetrichelvan, Y.-H. Lai, K. F. Mok, *Eur. J. Inorg. Chem.* **2004**, 2086–2095.
[12] A. N. Khlobystov, A. J. Blake, N. R. Champness, D. A. Lemenovskii, A. G. Majouga, N. V. Zyk, M. Schröder, *Coord. Chem. Rev.* **2001**, *222*, 155–192.
[13] S.-L. Zheng, M.-L. Tong, X.-M. Chen, *Coord. Chem. Rev.* **2003**, *246*, 185–202.
[14] S. Sailaja, M. V. Rajasekharan, *Inorg. Chem.* **2000**, *39*, 4586–4590.
[15] Y. J. K. Ok-Sang Jung, Y.-A. Lee, H. K. Chae, H. G. Jang, J. Hong, *Inorg. Chem.* **2001**, *40*, 2105–2110.
[16] M. Hong, W. Su, R. Cao, M. Fujita, J. Lu, *Chem. Eur. J.* **2000**, *6*, 427–431.
[17] S.-L. Zheng, M.-L. Tong, R.-W. Fu, X.-M. Chen, S.-W. Ng, *Inorg. Chem.* **2001**, *40*, 3562–3569.
[18] R. P. Feazell, C. E. Carson, K. K. Klausmeyer, *Inorg. Chem.* **2005**, *44*, 996–1005.
[19] K. K. Klausmeyer, R. P. Feazell, J. H. Reibenspies, *Inorg. Chem.* **2004**, *43*, 1130–1136.
[20] C. Seward, J. Chan, D. Song, S. Wang, *Inorg. Chem.* **2003**, *42*, 1112–1120.
[21] Y. Kang, S. S. Lee, K.-M. Park, S. H. Lee, S. O. Kang, J. Ko, *Inorg. Chem.* **2001**, *40*, 7027–7031.
[22] D. L. Reger, R. F. Semeniuc, M. D. Smith, *Inorg. Chem.* **2001**, *40*, 6545–6546.
[23] S. Sailaja, M. V. Rajasekharan, *Inorg. Chem.* **2003**, *42*, 5675–5684.
[24] P. L. Caradoc-Davies, L. R. Hanton, W. Henderson, *J. Chem. Soc., Dalton Trans.* **2001**, 2749–2755.
[25] V. J. Catalano, S. J. Horner, *Inorg. Chem.* **2003**, *42*, 8430–8438.
[26] R. J. Puddephatt, *Coord. Chem. Rev.* **2001**, *216–217*, 313–332.
[27] P. Pyykkö, *Chem. Rev.* **1997**, *97*, 597–636.
[28] A. Codina, E. J. Fernández, P. G. Jones, A. Laguna, J. M. López-de-Luzuriaga, M. Monge, M. E. Olmos, J. Pérez, M. A. Rodríguez, *J. Am. Chem. Soc.* **2002**, *124*, 6781–6786.

[29] E. J. Fernández, J. M. López-de-Luzuriaga, M. Monge, M. E. Olmos, J. Pérez, A. Laguna, A. A. Mohamed, J. John, P. Fackler, *J. Am. Chem. Soc.* **2003**, *125*, 2022–2023.
[30] R. E. Bachman, M. S. Fioritto, S. K. Fetics, T. M. Cocker, *J. Am. Chem. Soc.* **2001**, *123*, 5376–5377.
[31] D. E. Harwell, M. D. M. B. Knobler, F. A. L. Anet, M. F. Hawthorne, *J. Am. Chem. Soc.* **1996**, *118*, 2679–2685.
[32] V. J. Catalano, M. A. Malwitz, *Inorg. Chem.* **2003**, *42*, 5483–5485.
[33] A. A. Mohamed, L. M. Pérez, J. John, P. Fackler, *Inorg. Chim. Acta* **2005**, *358*, 1657–1662.
[34] C.-M. Che, M.-C. Tse, M. C. W. Chan, K.-K. Cheung, D. L. Phillips, K.-H. Leung, *J. Am. Chem. Soc.* **2000**, *122*, 2464–2468.
[35] Q.-M. Wang, T. C. W. Mak, *J. Am. Chem. Soc.* **2001**, *123*, 7594–7600.
[36] M. A. Omary, T. R. Webb, Z. Assefa, G. E. Shankle, H. H. Patterson, *Inorg. Chem.* **1998**, *37*, 1380–1386.
[37] H. Abbas, A. L. Pickering, D.-L. Long, P. Kögerler, L. Cronin, *Chem. Eur. J.* **2005**, *11*, 1071–1078.
[38] P. Pyykko, N. Runeberg, F. Mendizabal, *Chem. Eur. J.* **1997**, *3*, 1451–1457.
[39] P. Pyykko, N. Runeberg, F. Mendizabal, *Chem. Eur. J.* **1997**, *3*, 1458–1465.
[40] H. L. Hermann, G. Boche, P. Schwerdtfeger, *Chem. Eur. J.* **2001**, *7*, 5333–5342.
[41] E. J. Fernández, J. M. López-de-Luzuriaga, M. Monge, M. A. Rodríguez, M. Olga Crespo, C. Gimeno, A. Laguna, P. G. Jones, *Inorg. Chem.* **1998**, *37*, 6002–6006.
[42] A. Bacher, C. H. Erdelen, W. Paulus, H. Ringsdorf, H.-W. Schmidt, P. Schuhmacher, *Macromolecules* **1999**, *32*, 4551–4557.
[43] J. A. Jiménez, R. M. Claramunt, O. Mó, M. Yáñez, F. Wehrmann, G. Buntkowsky, H.-H. Limbach, R. Goddard, J. Elguero, *Phys. Chem. Chem. Phys.* **1999**, *1*, 5113–5120.
[44] Y. Ba, D. Chagolla, *J. Phys. Chem. B* **2002**, *106*, 5250–5257.
[45] G. M. Sheldrick, *SADABS*, University of Göttingen, Göttingen, Germany, **1997**.

Received: March 11, 2005
Published Online: July 6, 2005

